Size Dependence of Negative Trion Auger Recombination in Photodoped CdSe Nanocrystals

ARTICLE *in* NANO LETTERS · DECEMBER 2013

Impact Factor: 13.59 · DOI: 10.1021/nl4041675 · Source: PubMed

NANO LETTERS

Letter

pubs.acs.org/NanoLett

Size Dependence of Negative Trion Auger Recombination in Photodoped CdSe Nanocrystals

Alicia W. Cohn, Jeffrey D. Rinehart, Alina M. Schimpf, Amanda L. Weaver, and Daniel R. Gamelin*

Department of Chemistry, University of Washington, Seattle, Washington 98195-1700, United States

Supporting Information

ABSTRACT: We report a systematic investigation of the size dependence of negative trion (T^-) Auger recombination rates in free-standing colloidal CdSe nanocrystals. Colloidal n-type CdSe nanocrystals of various radii have been prepared photochemically, and their trion decay dynamics have been measured using time-resolved photoluminescence spectroscopy. Trion Auger time constants spanning 3 orders of magnitude are observed, ranging from 57 ps (radius R = 1.4 nm) to 2.2 ns (R = 3.2 nm). The data reveal a substantially stronger size dependence than found for bi- or multiexciton Auger recombination in CdSe or other semiconductor nanocrystals, scaling in proportion to $R^{4.3}$.

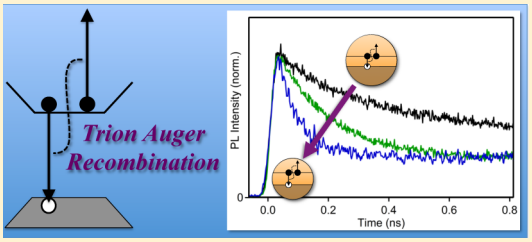

KEYWORDS: *Auger recombination, trion, n-type, quantum dot, nanocrystal*

Semiconductor nanocrystals possessing one or more "extra" charge carriers are central to many nascent quantum-dot technologies, from quantum computers[1,2] to solar cells.[3,4] In addition to changing the electrical and spin properties of quantum dots, the extra charge carriers have a dramatic impact on nanocrystal excited-state relaxation dynamics. Photoexcitation of an n- or p-doped nanocrystal with just one extra delocalized carrier creates a trion state (T^- or T^+, respectively) that can relax rapidly via a so-called Auger recombination[5] in which the energy of the photogenerated electron–hole pair is transferred nonradiatively to the extra carrier.

Trion Auger recombination has long been suspected to play a major role in nanocrystal photoluminescence (PL) intermittency,[6−11] and recent work has suggested that trion Auger recombination in photoionized nanocrystals may have contributed to overestimated carrier-multiplication yields.[12,13] Trion Auger recombination has also been implicated in efficiency droop in nanocrystal light-emitting diodes (LEDs),[14] as proposed for bulk LEDs.[15] Given the enormous scrutiny of photophysical processes linked to trions in these contexts, there has been remarkably little direct characterization of trion Auger recombination in colloidal semiconductor nanocrystals. For example, only recently were any negative-trion decay times of colloidal n-type nanocrystals directly measured, in this case for electrochemically reduced CdSe/CdS nanocrystals (R(core) = ∼2 nm, R(core/shell) = ∼3 nm) affixed to electrode surfaces.[8] These measurements revealed T^- Auger recombination an order of magnitude slower than biexciton Auger recombination and hence not sufficiently fast compared to radiative decay to account for nanocrystal intermittent dark states. Transient trion formation has been correlated with the occurrence of "gray" states in PL blinking traces,[16−18] confirming the importance of this motif in nanocrystal PL intermittency.

Where examined, multicarrier Auger recombination is generally greatly accelerated in nanocrystals,[19−21] likely because of the importance of interfaces for momentum conservation. For example, biexciton Auger recombination rates scale roughly with the inverse nanocrystal volume, the same size dependence has been observed for multiexcitons,[22] and a linear scaling with volume has been assumed for trions as well.[14,17,23] This size dependence can be qualitatively understood in terms of increasing high-k components of the charge-carrier wave functions with increasing confinement,[24] but systematic data characterizing trion Auger recombination in different sized nanocrystals are not available for quantitative assessment. A thorough and systematic experimental characterization of trion Auger rates in semiconductor nanocrystals would provide valuable input for quantitative theoretical descriptions of the critical factors regulating Auger rates in quantum dots in general. To this end, we report here the size dependence of T^- Auger recombination rates in free-standing colloidal n-type CdSe nanocrystals prepared via photochemical oxidation of the sacrificial hole quencher $Li[Et_3BH]$.[25] The resulting data agree well with the literature data[8] for CdSe/CdS nanocrystals at R ∼ 3 nm but show a significantly stronger size dependence than biexciton or multiexciton Auger recombination when other sizes are considered. The implications of these new data are discussed.

Figure 1 plots absorption and PL spectra of representative CdSe nanocrystals used in this study. The dotted curves show features characteristic of high-quality hot-injection CdSe nanocrystals. The solid curves show spectra of the same nanocrystals following growth of thin (∼1 monolayer) ZnS

Received: November 10, 2013
Revised: December 9, 2013
Published: December 16, 2013

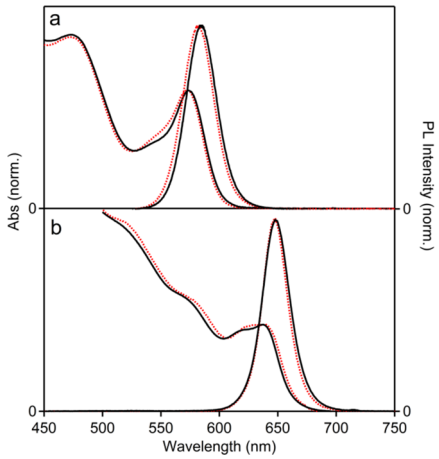

Figure 1. Room-temperature absorption and photoluminescence spectra of representative colloidal CdSe core nanocrystals (dotted red) and CdSe/ZnS core/shell nanocrystals (solid black). (a) R = 1.8 nm core nanocrystals, and (b) R = 3.2 nm core nanocrystals. Spectra have been normalized to facilitate comparison.

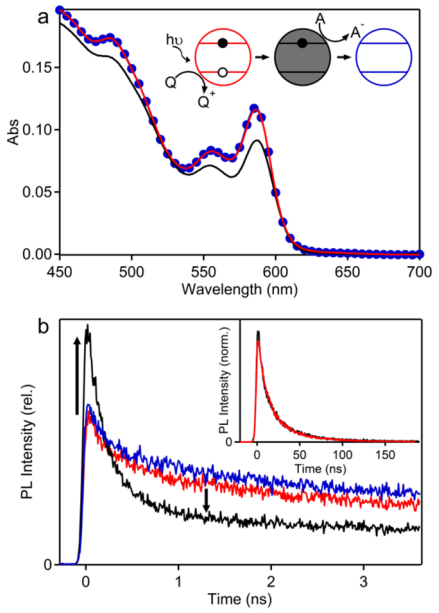

Figure 2. (a) Room-temperature absorption spectra of colloidal R = 2 nm CdSe/ZnS nanocrystals before photodoping (red), after photodoping (black), and after reoxidation by exposure to air (blue circles). The inset summarizes the photodoping and reoxidation processes schematically. (b) Room-temperature neutral-exciton and trion PL decay curves associated with the three absorption spectra in (a). The inset shows the complete PL decay curves measured before (red) and after (black) photodoping, normalized at 50 ns. The arrows indicate intensity changes upon photodoping.

shells. The spectra are not significantly altered upon shell growth, as expected. Such ZnS shells eliminate nonradiative decay channels without relaxing carrier confinement, which would complicate analysis of the Auger dependence on nanocrystal radius. The remaining experiments described in this paper were all performed using similar CdSe/ZnS core/shell nanocrystals, and the data were analyzed assuming an effective radius equal to that of the CdSe cores alone.

Colloidal *n*-type nanocrystals were prepared by photoexcitation of these CdSe/ZnS core/shell nanocrystals in the presence of the hole quencher, $Li[Et_3BH]$, as detailed previously[25] (see Methods). Under anaerobic conditions, this photochemical borohydride oxidation yields a stable population of colloidal nanocrystals possessing extra conduction-band electrons compensated by Li^+ and H^+ cations. These colloidal n-type nanocrystals are of high spectroscopic quality, making them well suited for further spectroscopic examination. Figure 2 shows a representative set of absorption spectra and PL decay curves measured before photodoping, after photodoping, and after reoxidation of the CdSe/ZnS nanocrystals in air. The decrease at the first absorption maximum upon photodoping is characteristic of partial occupancy of the conduction band by delocalized electrons.[26] Because the $1S_e$ orbital can be occupied by two electrons, reduction by two electrons per nanocrystal would yield a full absorption bleach.[26] The data in Figure 2a show ~20% absorption bleach at the first maximum, indicating an average number of conduction-band electrons per nanocrystal of $\langle n \rangle \sim 0.4$. For all measurements described here, photodoping was kept at $\langle n \rangle \ll 1$ to exclude the possibility of doubly reduced nanocrystals. The photodoped nanocrystals are readily reoxidized upon opening the cuvette to air. Figure 2a shows that the absorption spectrum of the reoxidized nanocrystals nicely overlays that collected prior to photodoping, indicating well-behaved reversible photodoping without sample degradation.[25]

In the time domain, the PL decay measured prior to photodoping is dominated by a $\tau \sim 17$ ns component similar to the radiative lifetime expected[27] at room temperature. A small, fast-decay component (τ = 0.57 ns) is also observed, attributable to nonradiative processes. For all samples reported here, the exciton PL decay prior to photodoping is similarly multiexponential, which is common among CdSe nanocrystals.[28,29] Upon photodoping (confirmed by the exciton bleach in Figure 2a), the PL decay of this same sample shows an increase in intensity at short times that decays relatively rapidly (τ = 0.22 ns), followed by a slow decay process. The inset of Figure 2b plots the PL decay curves of the neutral and photodoped nanocrystals over a long time window, normalized at t = 50 ns. The two decay curves overlay one another well, confirming that the long time component in the photodoped sample is simply due to decay of neutral nanocrystals in the ensemble having $\langle n \rangle \ll 1$. To ensure measurement of solely trion decay times, and not decay of nanocrystals containing multiple electrons, all measurements reported here were performed under conditions where neutral nanocrystals were clearly detected in the PL decay. In addition, nanocrystals possessing more than one extra conduction electron have a second PL peak at higher energy than that observed from the neutral exciton or negative trion. This peak is attributed to recombination of electrons from the $1P_e$ conduction level with valence-band holes,[30] and PL spectra were therefore used to verify that this feature was not present under the conditions used for the trion lifetime measurements (see Supporting Information).

Figure 2b also shows that the PL decay of the reoxidized nanocrystals does not perfectly overlay that of the same nanocrystals prior to photodoping. Frequently, the PL intensity recovers completely only after extended exposure to air, and initial recovery was found to vary from sample to sample (see Supporting Information). The source of this variability is not clear, but it may arise from slow reoxidation of deeply trapped electrons, or possibly from surface restructuring of the photodoped nanocrystals. Importantly, even when the PL intensity does not recover fully, the PL decay kinetics do,

dx.doi.org/10.1021/nl4041675 | *Nano Lett.* 2014, 14, 353−358

indicating that the lost PL intensity is associated with nonradiative processes that are faster than our PL instrument response time (~15 ps). We have observed that the intensity irreversibility can be mitigated, if not completely suppressed, by addition of surface-passivating trioctylphosphine ligands to the nanocrystal solution before photodoping. These observations suggest that the intensity irreversibility may relate to creation of new surface traps upon photodoping.

The PL decay data in Figure 2b are very similar to those reported for CdSe/CdS nanocrystals reduced electrochemically.[8] The increased intensity at short times upon reduction is attributable to the increased radiative decay rate of the trion (about twice that of the exciton). The much faster decay of this PL is attributable to trion Auger recombination. To quantify the trion lifetimes from these data, we first subtracted the PL decay signal from the neutral nanocrystals present in the ensemble. Here, the PL decay measured before photodoping was fitted at long times with a single-exponential function to give the dominant component of the neutral exciton lifetime (τ_{Xslow}). With τ_{Xslow} held constant, the neutral exciton PL decay at short times was then fitted to a biexponential function (eq 1), where τ_{Xfast} accounts for faster nonradiative decay processes of the neutral nanocrystals. This biexponential fit reasonably reproduces the experimental multiexponential decay over all times. The trion lifetime (τ_{T^-}) was then determined by fitting the PL decay of the photodoped nanocrystals with eq 2, keeping τ_{Xslow}, τ_{Xfast}, and A_{slow}/A_{fast} fixed to account for the remaining neutral nanocrystals. This procedure is equivalent to simply subtracting the PL decay of the residual neutral nanocrystals and fitting the trion decay with a single exponential.

$$I(t) = A_{slow}\exp\left(\frac{-t}{\tau_{Xslow}}\right) + A_{fast}\exp\left(\frac{-t}{\tau_{Xfast}}\right) \quad (1)$$

$$I(t) = c\left[A_{slow}\exp\left(\frac{-t}{\tau_{Xslow}}\right) + A_{fast}\exp\left(\frac{-t}{\tau_{Xfast}}\right)\right] + A_{T^-}\exp\left(\frac{-t}{\tau_{T^-}}\right) \quad (2)$$

As described by eq 3, τ_{T^-} is determined by trion radiative decay and Auger recombination dynamics. The trion's radiative decay time constant (τ_{T^-rad}) can be estimated from τ_{Xslow} based on the empirical ratio of $\tau_{Xrad}/\tau_{T^-rad} = 2.2$,[8] and its Auger time constant (τ_{A^-}) is then determined using eq 3. This analysis thus assumes that no other nonradiative processes appear upon photodoping, disappear upon reoxidation, *and* occur on the same time scale as the trion Auger recombination, where they would contaminate the Auger recombination dynamics. This assumption is not easily justified a priori, but its validity is supported by the collection of data over different nanocrystal radii (vide infra) and by comparison with literature data.

$$\frac{1}{\tau_{T^-}} = \frac{1}{\tau_{A^-}} + \frac{1}{\tau_{T^-_{Rad}}} \quad (3)$$

Figure 3 plots the PL decay of three photodoped ($\langle n\rangle \ll 1$) CdSe/ZnS nanocrystal samples with different radii. The curves are all normalized at $t = 0$ ns to illustrate the increasingly rapid trion decay with decreasing nanocrystal radius (arrow). Following the procedure outlined above, τ_{A^-} was determined for each sample, as well as for several other samples with

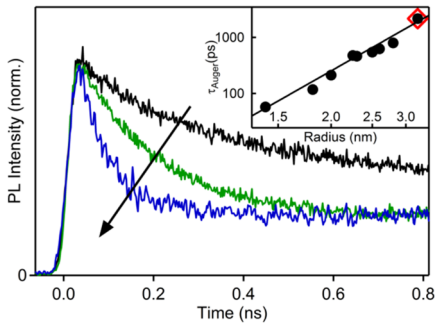

Figure 3. Room-temperature photoluminescence decay curves measured for colloidal photodoped CdSe/ZnS nanocrystals of different radii, R, normalized at $t = 0$ ns. Decay curves are shown for $R = 1.4$ nm (blue), 2.0 nm (green), and 3.2 nm (black), and the arrow shows the decreasing trion lifetime with decreasing R. Note that each sample has a different fraction of nanocrystals with no electrons, so the decay curves do not all approach precisely the same long-time asymptote. The inset shows a double-log plot of τ_{A^-} versus R for the entire series of CdSe/ZnS nanocrystals measured here following photodoping (●). The $R = 3.2$ nm nanocrystals were also examined following chemical reduction using Na[biphen] (red ◊). The line in the inset shows the best fit to the data using eq 4, which yields $p = 4.3$.

various radii (see Supporting Information). The inset shows a double-log plot of τ_{A^-} versus R for the entire set of samples. τ_{A^-} spans 3 orders of magnitude, ranging from 57 ps ($R = 1.4$ nm) to 2.2 ns ($R = 3.2$ nm). The largest CdSe nanocrystals in Figure 3 were also reduced using sodium biphenyl (Na[biphen]) as the reductant, and τ_{A^-} determined in the same way is also plotted in the inset. The chemically and photochemically reduced nanocrystals show indistinguishable τ_{A^-} values. These data reveal a strong and well-behaved dependence of the T^- Auger recombination time on nanocrystal radius. For this entire data set, a best fit to eq 4 yields $p = 4.3$. This exponent is robust with respect to the method of data analysis. For example, very similar results are obtained when $\tau_{Xrad}/\tau_{T^-rad}$ is assumed to equal 2.0. Likewise, simply fitting the raw PL decay data of the photodoped nanocrystals (e.g., Figure 3) with a single exponential function and an intensity offset also yields the same result (see Supporting Information). The insensitivity of the exponent ($p = 4.3$) to the method of data analysis reflects the fact that trion Auger recombination is the dominant feature of the photodoped nanocrystal PL decay data in this time window.

$$\tau_{Auger} = AR^p \quad (4)$$

There is very little scatter among the data in Figure 3 (inset), despite having used two different CdSe nanocrystal syntheses and two different methods of nanocrystal *n*-doping (photochemical and chemical), and having samples showing different extents of competing nonradiative neutral-exciton decay. For example, two nanocrystals with $R \approx 2.3$ nm synthesized by the methods of refs 31−33 showed significantly different neutral-exciton PL decay dynamics, with $\tau_{Xslow} = 24$ versus 16 ns, respectively (see Supporting Information), but their τ_{A^-} values differed by only ~5%. Similarly, the τ_{A^-} values measured for the same chemically and photochemically reduced $R = 3.2$ nm nanocrystals were indistinguishable (Figure 3, inset). These results provide additional strong support for the robustness of the analysis described above. Specifically, the method of n-doping and changes in other nonradiative relaxation processes upon n-doping do not significantly impact the trion decay

dx.doi.org/10.1021/nl4041675 | *Nano Lett.* 2014, 14, 353−358

measurements. For example, filling (reduction) of midgap traps is known to occur during this photodoping.[25] Although such filling could conceivably introduce competing "trap-assisted" Auger recombination processes,[34] the new trap-centered recombination observed following photodoping of these CdSe nanocrystals occurs much faster than the trion Auger recombination. Consequently, trap reduction causes an overall decrease in PL intensity without obscuring the trion decay dynamics.[25]

The data in Figure 3 offer the opportunity to compare the experimental size dependence of a trion's Auger recombination with those of other multicarrier Auger recombination processes for the first time. Figure 4 plots the negative trion τ_{A^-} values

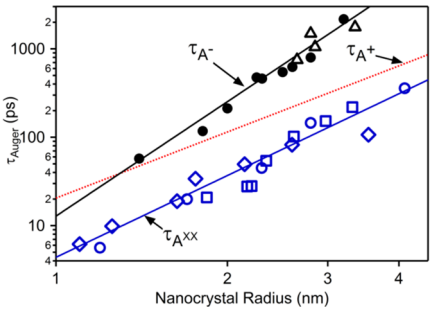

Figure 4. Double-log plot of Auger recombination time constants versus CdSe nanocrystal radius, including experimental negative trion (τ_{A^-}) and biexciton (τ_A^{XX}) Auger time constants, and projected positive trion (τ_{A^+}) Auger time constants: τ_{A^-} from this work (●); Literature τ_{A^-} (Δ, ref 8); Literature τ_A^{XX} (blue symbols: ○ (ref 22), ◊ (ref 35), and □ (ref 36)). The size dependence of τ_{A^+} (red dotted line) is calculated from the best fits of eq 4 to the experimental τ_{A^-} data (p = 4.3) and the literature τ_A^{XX} data (p = 3.0) using eq 5, and yields p = 2.5 from eq 4

from this work together with τ_{A^-} values estimated from analogous literature data.[8] At similar R, the τ_{A^-} values from the present work agree remarkably well with those deduced from trion decay data reported[8] for electrochemically reduced $R \sim 3$ nm CdSe/CdS nanocrystals (assuming the full core/shell radius to be the effective radius, and analyzed as described above). This agreement lends further credence to the analysis applied here. Figure 4 also plots literature[22,35,36] biexciton Auger recombination times (τ_A^{XX}) versus R for similar CdSe nanocrystals. As reported previously,[20,22,35,36] fitting these τ_A^{XX} data to eq 4 yields p = 3.0.

Just as the precise origins of the p = 3.0 size dependence of τ_A^{XX} are not trivially understood,[20] it is not obvious why τ_{A^-} scales with p = 4.3. Trion Auger recombination rates are governed by Fermi Golden Rule considerations[24] and are expected to depend on intercarrier Coulomb interaction strengths, carrier surface probability densities, shapes of the confinement potentials, confinement-induced state mixing, and densities of states fulfilling the resonance criteria, all of which should vary with nanocrystal size. A stronger size dependence of the resonant density of states for trion versus biexciton Auger recombination, for example, might manifest itself in the observed stronger size dependence of τ_{A^-} than of τ_A^{XX}. It is not known which, if any, of these factors is dominant.

In simple core-only nanocrystals, the biexciton Auger recombination time constant has been related to positive and negative trion Auger recombination time constants based on statistical considerations as described by eq 5.[37] There is still no consensus about the relative magnitudes or size dependence of τ_{A^-}, τ_{A^+}, and τ_A^{XX} in CdSe nanocrystals, however. For example, some calculations[37] suggest $\tau_{A^-} \approx \tau_{A^+}$, and hence $\tau_{A^-}/\tau_A^{XX} \approx 4$ (from eq 5), but others[38] suggest a significantly smaller ratio of $\tau_{A^-}/\tau_A^{XX} \approx 2.3$. From the experimental size dependence of τ_{A^-} measured here, it is evident that τ_{A^-} and τ_A^{XX} depend differently on R (p = 4.3 vs 3.0), and hence τ_{A^-}/τ_A^{XX} must also be size dependent. From these data, τ_{A^-}/τ_A^{XX} decreases from ~13 at R = 3.3 nm to ~5 at R = 1.4 nm. A size dependence of τ_{A^-}/τ_A^{XX} in CdSe nanocrystals has been predicted theoretically, in which τ_{A^-}/τ_A^{XX} = 3.1 for R = 1.39 nm nanocrystals and 2.5 for R = 1.92 nm nanocrystals, both in a toluene dielectric.[38] Given literature τ_A^{XX} data, these computed ratios imply values of τ_{A^-} = 37 and 81 ps, respectively, which represent a somewhat smaller size dependence (p = 2.4) than we observe experimentally (p = 4.3, Figure 3).

$$\frac{1}{\tau_{A^{XX}}} = \frac{2}{\tau_{A^-}} + \frac{2}{\tau_{A^+}} \quad (5)$$

Other systematic experimental measurements of the size dependence of trion Auger recombination rates do not exist. The strong trion-Auger size dependence observed here is consistent with previous reports of slow trion Auger recombination in colloidal core/thick-shell nanocrystals,[23,39,40] colloidal dot-in-rod nanocrystals,[41] and self-assembled quantum dots,[42] all possessing much greater internal volumes, but other factors including reduced electron–hole overlap and interface gradation are undoubtedly also important in these more-complex nanostructures. To our knowledge, the only analogous data are available from transient cathodoluminescence decay measurements on nanocrystal films of three CdSe/ZnS samples and analysis involved deconvolution of overlapping luminescence from multiple species.[43] These data show a smaller size dependence of τ_{A^-} than observed here, corresponding to $p \sim$ 1.1. The origin of this difference is unclear. We note that the simplicity of the photodoping and photoluminescence approach reported in the present study is favorable for allowing unambiguous identification and analysis of negative trions in colloidal CdSe nanocrystals.

If eq 5 is valid, then positive trion Auger times (τ_{A^+}) can also be predicted from the trion and biexciton Auger data, and this result is plotted in Figure 4 along with the other data. For all experimental radii investigated here, τ_{A^+} is predicted to be smaller than τ_{A^-}, but it also shows a smaller size dependence (p = 2.5 from eq 4) than either τ_{A^-} or τ_A^{XX}. Both observations would be consistent with expectations from the greater density of states in the valence bands of II–VI semiconductors than in their conduction bands, assuming a greater density of states results in a lesser sensitivity to changes in the density of states.[44] Because of its strong size dependence, τ_{A^-} may even become faster than τ_{A^+} at very small R, according to eq 5. As stressed previously,[8] however, eq 5 neglects four-particle processes in biexciton Auger recombination, in which the energy from the recombining exciton is partitioned between the electron and hole of the remaining exciton. Stable p-doped colloidal CdSe nanocrystals have not been prepared experimentally, and without independently measuring τ_{A^+}, it is not possible to determine the validity of eq 5. A value of τ_{A^+} = 1.1 ns has been reported for CdSe/CdS nanocrystals (core R = 1.8 nm, core/shell R = 4–5 nm), however, measured by variable-repetition-rate photoluminescence spectroscopy,[45] and for the same nanocrystals, τ_A^{XX} = 0.40 ns and τ_{A^-} = 2.3 ns were reported. Although a direct comparison of these data with those

dx.doi.org/10.1021/nl4041675 | Nano Lett. 2014, 14, 353–358

presented in Figure 4 is complicated by the influence of the thick CdS shells in the former, the data are consistent with eq 5.

Finally, the data presented here also imply a strong size dependence of trion PL quantum yields. From analysis of experimental decay dynamics, $R \sim 3$ nm CdSe/CdS nanocrystals have been predicted to have negative trion PL quantum yields as large as 10−15%.[8] The data here support this proposal but also suggest that the maximum PL quantum yields of negative trions should decrease rapidly to <1% at the smallest radii investigated here ($R = 1.4$), simply because of the strong size dependence of τ_{A^-} (see Supporting Information). The strong size dependence of τ_{A^-} may thus cause an order of magnitude variation in the brightness of "gray" states observed during nanocrystal intermittency, depending on nanocrystal radius. Awareness of this τ_{A^-} size dependence may therefore inform interpretations of the microscopic origins of these gray states.

In summary, the dependence of negative trion Auger recombination on nanocrystal radius has been measured for free-standing colloidal n-doped CdSe nanocrystals prepared photochemically. Negative trion Auger recombination accelerates rapidly with decreasing nanocrystal radius, with τ_{A^-} proportional to $R^{4.3}$. This scaling contrasts with the universal[20] R^3 scaling of bi- and multiexciton Auger recombination, and it implies a weaker size dependence of Auger recombination in the as-yet inaccessible CdSe positive trion. These results provide an experimental basis for the development and testing of theoretical descriptions of trion Auger recombination dynamics in CdSe and related semiconductor nanocrystals. Beyond the specific CdSe results presented here, these findings demonstrate the utility of photodoping[25] as an approach for exploring the unique physical properties of high-quality electronically doped colloidal semiconductor nanocrystals.

Methods. Colloidal CdSe nanocrystals were synthesized by hot-injection following literature procedures.[31−33] $R = 3.2$, 2.5, 2.3, and 2.0 nm nanocrystals were synthesized following the procedures detailed in refs 31 and 32. $R = 2.8$, 2.6, 2.5, and 1.8 nm nanocrystals were synthesized by adapting the procedures of ref 33. For this, 0.05 g of CdO and 0.5 g of stearic acid were degassed in a three neck flask at 100 °C after which the temperature was raised to 270 °C and cadmium stearate was formed. The temperature was lowered to 100 °C and 2.5 g of hexadecylamine and 2 g of trioctylphosphine oxide (TOPO) were added to the flask. This mixture was degassed for 30 min before the temperature was raised to 330 °C and a solution of 0.15 g of Se in 1.5 mL of trioctylphosphine (TOP) was swiftly injected. The growth time was adjusted to between 1 and 3 min to reach the desired nanocrystal sizes. Nanocrystals with $R = 1.4$ nm were obtained following the same procedure but by adding 16 g of octadecene to the cation reaction flask to be degassed along with the CdO and stearic acid. For all nanocrystals, ZnS shells were grown using the SILAR method.[46]

All spectroscopic data were collected at room temperature on colloidal suspensions of nanocrystals. Absorption spectra collected using a Cary 500 spectrophotometer (Varian) and nanocrystal radii were estimated from these spectra using the empirical relationship presented in ref 47. For photoluminescence measurements, a sealable cuvette containing 2 mL of nanocrystal solution (band gap absorption = 0.1−0.2) with ∼2 mg of extra 99% TOPO as well as ∼0.1 mL of TOP if necessary (see main text) was prepared in a N_2 atmosphere glovebox. This solution was used for neutral-exciton photoluminescence, luminescence decay, and absorption measurements and then brought back into the glovebox. Nanocrystal photodoping was then performed following the procedures detailed in ref 25. Briefly, 10 μL of 1 M lithium triethylborohydride ($Li[Et_3BH]$) in THF (used as received from Sigma-Aldrich) was added to 1 mL of toluene, and 10−20 μL of this 0.01 M $Li[Et_3BH]$ solution was added to the nanocrystal solution. For all nanocrystals, exposure to ambient room lights was sufficient to photodope the nanocrystals within ∼3 min with the exception of the smallest ($R = 1.4$ nm) nanocrystals, which were instead illuminated using a Hg/Xe arc lamp equipped with a 450 nm cutoff filter for ∼5 min. For chemical reduction, 60 μL of ∼0.1 M sodium biphenyl radical solution (Na[biphen]) was added instead of $Li[Et_3BH]$. Photoluminescence decay curves were measured by exciting the nanocrystals with the frequency-doubled output of a Ti:sapphire laser at a 500 kHz repetition rate (400 nm, 150 fs pulse, 0.7 nJ/pulse). Decay curves were recorded using a monochromator and streak camera with an instrument response function of ∼15 ps. Luminescence spectra were collected using an unfocused 405 nm laser diode (∼5 mW) for excitation and an OceanOptics 2000+ spectrometer for detection.

■ ASSOCIATED CONTENT

Supporting Information

Additional absorption, PL, and time-resolved PL data, streak-camera data, tabulated nanocrystal data including energy gaps, radii, PL time constants and Auger recombination time constants, and estimated trion PL quantum yields. This material is available free of charge via the Internet at http://pubs.acs.org.

■ AUTHOR INFORMATION

Corresponding Author

*E-mail: Gamelin@chem.washington.edu.

Notes

The authors declare no competing financial interest.

■ ACKNOWLEDGMENTS

Financial support from the U.S. National Science Foundation (DMR-1206221 to D.R.G., Graduate Research Fellowship DGE-1256082 to A.M.S.) and the Department of Energy (Energy Efficiency and Renewable Energy (DOE-EERE) Fellowship to J.D.R.) is gratefully acknowledged.

■ REFERENCES

(1) Loss, D.; DiVincenzo, D. P. *Phys. Rev. A* **1998**, *57*, 120.
(2) Awschalom, D. D.; Bassett, L. C.; Dzurak, A. S.; Hu, E. L.; Petta, J. R. *Science* **2013**, *339*, 1174.
(3) Nozik, A. J.; Beard, M. C.; Luther, J. M.; Law, M.; Ellingson, R. J.; Johnson, J. C. *Chem. Rev.* **2010**, *110*, 6873.
(4) Mora-Seró, I.; Giménez, S.; Fabregat-Santiago, F.; Gómez, R.; Shen, Q.; Toyoda, T.; Bisquert, J. *Acc. Chem. Res.* **2009**, *42*, 1848.
(5) Landsberg, P. T. *Recombination in Semiconductors*; Cambridge University Press: Cambridge, 1991.
(6) Chepic, D. I.; Efros, A. L.; Ekimov, A. I.; Ivanov, M. G.; Kharchenko, V. A.; Kudriavtsev, I. A.; Yazeva, T. V. *J. Lumin.* **1990**, *47*, 113.
(7) Efros, A. L. Auger Processes in Nanosize Semiconductor Crystals. In *Semiconductor Nanocrystals: from Basic Principles to Applications*; Efros, A. L., Lockwood, D. J., Tsybeskov, L., Eds.; Kluwer Academic: New York, 2003; p 52.
(8) Jha, P. P.; Guyot-Sionnest, P. *ACS Nano* **2009**, *3*, 1011.

(9) Zhao, J.; Nair, G.; Fisher, B. R.; Bawendi, M. G. *Phys. Rev. Lett.* **2010**, *104*, 157403.
(10) Rosen, S.; Schwartz, O.; Oron, D. *Phys. Rev. Lett.* **2010**, *104*, 157404.
(11) Califano, M. *J. Phys. Chem. C* **2011**, *115*, 18051.
(12) McGuire, J. A.; Sykora, M.; Joo, J.; Pietryga, J. M.; Klimov, V. I. *Nano Lett.* **2010**, *10*, 2049.
(13) Tyagi, P.; Kambhampati, P. *J. Chem. Phys.* **2011**, *134*, 094706.
(14) Bae, W. K.; Park, Y.-S.; Lim, J.; Lee, D.; Padilha, L. A.; McDaniel, H.; Robel, I.; Lee, C.; Pietryga, J. M.; Klimov, V. I. *Nat. Commun.* **2013**, *4*, 2661.
(15) Shen, Y. C.; Mueller, G. O.; Watanabe, S.; Gardner, N. F.; Munkholm, A.; Krames, M. R. *Appl. Phys. Lett.* **2007**, *91*, 141101.
(16) Song, N.; Zhu, H.; Jin, S.; Lian, T. *ACS Nano* **2011**, *5*, 8750.
(17) Qin, W.; Guyot-Sionnest, P. *ACS Nano* **2012**, *6*, 9125.
(18) Javaux, C.; Mahler, B.; Dubertret, B.; Shabaev, A.; Rodina, A. V.; Efros, A. L.; Yakovlev, D. R.; Liu, F.; Bayer, M.; Camps, G.; Biadala, L.; Buil, S.; Quelin, X.; Hermier, J.-P. *Nat. Nanotechnol.* **2013**, *8*, 206.
(19) Klimov, V. I. *J. Phys. Chem. B* **2006**, *110*, 16827.
(20) Robel, I.; Gresback, R.; Kortshagen, U.; Schaller, R. D.; Klimov, V. I. *Phys. Rev. Lett.* **2009**, *102*, 177404.
(21) Kobayashi, Y.; Nishimura, T.; Yamaguchi, H.; Tamai, N. *J. Phys. Chem. Lett.* **2011**, *2*, 1051.
(22) Klimov, V. I.; Mikhailovsky, A. A.; McBranch, D. W.; Leatherdale, C. A.; Bawendi, M. G. *Science* **2000**, *287*, 1011.
(23) Galland, C.; Ghosh, Y.; Steinbrück, A.; Hollingsworth, J. A.; Htoon, H.; Klimov, V. I. *Nat. Commun.* **2012**, *3*, 908.
(24) Cragg, G. E.; Efros, A. L. *Nano Lett.* **2010**, *10*, 313.
(25) Rinehart, J. D.; Schimpf, A. M.; Weaver, A. L.; Cohn, A. W.; Gamelin, D. R. *J. Am. Chem. Soc.* **2013**, DOI: 10.1021/ja410825c.
(26) Shim, M.; Guyot-Sionnest, P. *Nature* **2000**, *407*, 981.
(27) van Driel, A. F.; Allan, G.; Delerue, C.; Lodahl, P.; Vos, W. L.; Vanmaekelbergh, D. *Phys. Rev. Lett.* **2005**, *95*, 236804.
(28) Knowles, K. E.; McArthur, E. A.; Weiss, E. A. *ACS Nano* **2011**, *5*, 2026.
(29) Wang, H.; de Mello Donegá, C.; Meijerink, A.; Glasbeek, M. *J. Phys. Chem. B* **2006**, *110*, 733.
(30) Wang, C.; Wehrenberg, B. L.; Woo, C. Y.; Guyot-Sionnest, P. *J. Phys. Chem. B* **2004**, *108*, 9027.
(31) Carbone, L.; Nobile, C.; De Giorgi, M.; Della Sala, F.; Morello, G.; Pompa, P.; Hytch, M.; Snoeck, E.; Fiore, A.; Franchini, I. R.; Nadasan, M.; Silvestre, A. F.; Chiodo, L.; Kudera, S.; Cingolani, R.; Krahne, R.; Manna, L. *Nano Lett.* **2007**, *7*, 2942.
(32) Chen, O.; Zhao, J.; Chauhan, V. P.; Cui, J.; Wong, C.; Harris, D. K.; Wei, H.; Han, H.-S.; Fukumura, D.; Jain, R. K.; Bawendi, M. G. *Nat. Mater.* **2013**, *12*, 445.
(33) Peng, X.; Qu, L. *J. Am. Chem. Soc.* **2002**, *124*, 2049.
(34) Cohn, A. W.; Schimpf, A. M.; Gunthardt, C. E.; Gamelin, D. R. *Nano Lett.* **2013**, *13*, 1810.
(35) Achermann, M.; Hollingsworth, J. A.; Klimov, V. I. *Phys. Rev. B* **2003**, *68*, 245302.
(36) Pandey, A.; Guyot-Sionnest, P. *J. Chem. Phys.* **2007**, *127*, 111104.
(37) Wang, L.-W.; Califano, M.; Zunger, A.; Franceschetti, A. *Phys. Rev. Lett.* **2003**, *91*, 056404.
(38) Califano, M. *ACS Nano* **2011**, *5*, 3614.
(39) Spinicelli, P.; Buil, S.; Quélin, X.; Mahler, B.; Dubertret, B.; Hermier, J.-P. *Phys. Rev. Lett.* **2009**, *102*, 136801.
(40) Wang, X.; Ren, X.; Kahen, K.; Hahn, M. A.; Rajeswaran, M.; Maccagnano-Zacher, S.; Silcox, J.; Cragg, G. E.; Efros, A. L.; Krauss, T. D. *Nature* **2009**, *459*, 686.
(41) Rabouw, F. T.; Lunnemann, P.; van Dijk-Moes, R. J. A.; Frimmer, M.; Pietra, F.; Koenderink, A. F.; Vanmaekelbergh, D. *Nano Lett.* **2013**, *13*, 4884.
(42) Patton, B.; Langbein, W.; Woggon, U. *Phys. Rev. B* **2003**, *68*, 125316.
(43) Padilha, L. A.; Bae, W. K.; Klimov, V. I.; Pietryga, J. M.; Schaller, R. D. *Nano Lett.* **2013**, *13*, 925.
(44) If density-of-states differences underlie this asymmetry in CdSe, then IV−VI semiconductor nanocrystals would be expected to display a more similar size dependence of T^- and T^+ Auger recombination rates. Direct measurement of τ_{A^-} and τ_{A^+} size dependence in such systems would be desirable.
(45) Saba, M.; Aresti, M.; Quochi, F.; Marceddu, M.; Loi, M. A.; Huang, J.; Talapin, D. V.; Mura, A.; Bongiovanni, G. *ACS Nano* **2013**, *7*, 229.
(46) McLaurin, E. J.; Vlaskin, V. A.; Gamelin, D. R. *J. Am. Chem. Soc.* **2011**, *133*, 14978.
(47) Yu, W. W.; Qu, L.; Guo, W.; Peng, X. *Chem. Mater.* **2003**, *15*, 2854.